PNAS
www.pnas.org

Supplementary Information for

Pak2 kinase promotes cellular senescence and organismal aging

Jong-Sun Lee[1,5], Yan Mo[1,5], Haiyun Gan[1], Rebecca J. Burgess[4], Darren J. Baker[2,3], Jan M. van Deursen[2,3] and Zhiguo Zhang[1*]

[1]Institute for Cancer Genetics, Department of Pediatrics, Genetics and Development, Columbia University Irving Medical Center, New York, NY 10032, USA
[2]Departments of Pediatric and Adolescent Medicine and [3]Biochemistry and Molecular Biology, Mayo Clinic, Rochester, MN 55905, USA
[4]Children's Research Institute and the Department of Pediatrics, University of Texas Southwestern Medical Center, Dallas, TX 75390, USA
[5]These author contribute equally to this work

Zhiguo Zhang
Email: zz2401@cumc.columbia.edu

This PDF file includes:

Supplementary Information

SI Materials and Methods

Cell culture and gene transfer

IMR90 (ATCC) cells were grown in DMEM medium (Cellgro) supplemented with 10% fetal bovine serum (Sigma) and 1% penicillin/streptomycin (GIBCO), maintained at 37 ºC with 5% CO_2. Oncogene-induced senescence was performed as described previously (1-3). A retrovirus expressing a tamoxifen-inducible pLNC-neo ER::H-RasV^{12} construct was packaged in Phoenix cells and transduced into IMR90 cells following protocols previously described (4). Transduced cells were grown in the presence of 500 μg/mL G418. Expression of H-RasV^{12} was induced with 100 nM 4OHT (Sigma-Aldrich). The shRNAs against Pak2 were purchased from Sigma-Aldrich (shPak2#1:TRCN0000002115; shPak2# 2:TRCN0000002116). Lentiviral particles were produced using HEK293T cells.

Generation and culturing of MEFs

Since complete knockout of Pak2 in mice is embryonic lethal, we generated Pak2 knockdown mice using a gene-trap strategy. Mice with Pak2 depletion using this strategy are viable (H/H refers to animals homozygous for the gene trap allele). *BubR1*$^{+/H}$ mice were generously provided by Dr. Jan. van Deursen (5). We generated *Pak2*$^{+/H}$;*BubR1*$^{+/H}$ mice and then intercrossed *Pak2*$^{+/H}$;*BubR1*$^{+/H}$ mice to generate experimental cohorts of *BubR1*$^{H/H}$;*Pak2*$^{H/H}$ mice. Our control cohorts included *Pak2*$^{+/+}$;*BubR1*$^{H/H}$ littermate mice. We intercrossed *Pak2*$^{+/H}$ mice to derive *Pak2*$^{+/+}$, *Pak2*$^{+/H}$, and *Pak2*$^{H/H}$ MEFs, which were generated from trypsinized carcasses of 13.5-day-old embryos as previously described (6). They were cultured in 20% oxygen to induce senescence by oxidative stress, frozen at

P2 and P3 and used for experimentation at the indicated passages (P3, P5, and P7, n=3 MEF lines per genotype).

Histology

We fixed dissected tissues for histology in 10% formalin, processed them and embedded them in paraffin. We sliced 5μm sections of all tissues and stained them with hematoxylin and eosin using standard procedures. For histological evaluation of cataracts, 4-month-old eye tissue was embedded and sectioned through the middle of the lens. The number of cells that had posteriorly located epithelial cells was counted (n = 4 lenses per genotype). Measurements of fat cell cross sectional area were performed on cross-sections of paraffin-embedded IAT from 4-month-old mice (n = 4 per genotype). A total of 50 random cells per sample were measured using ImageJ software.

Body fat composition analyses

Measurements of body weight and IAT were performed on 16-week-old mice. At baseline and the end of the study in a subset of about 10 mice per genotype, lean mass and fat mass of individual mice are quantified using quantitative nuclear magnetic resonance and normalized relative to body weight.

Western blotting and antibodies

To perform Western blot analyses, SDS-PAGE gels were transferred onto nitrocellulose membranes (Bio-Rad). The membranes were blocked in Tris-buffered saline containing 5% (w/v) skim milk powder and then probed with the various antibodies: The following

commercial antibodies were used at the stated dilutions: Pak2 (No. 2608, Cell Signaling, 1:1000); α-tubulin (DSHB, 12G10, 1:5000); p16 (sc-468, Santa Cruz, 1:1000); H-RAS (Santa Cruz Biotechnology, sc-29, 1:1000). HIRA (Millipore, WC119, 1:1000).

RNA-seq and Quantitative real-time PCR

Total RNA was extracted from cells and tissue using the Quiagen miRNeasy Mini Kit for RNA-seq library preparation or quantitative RT-PCR (qRT-PCR) as the manufacturer described. RNA-seq libraries were prepared with Ovation RNA-seq system v2 kit (NuGEN) according to the manufacturer's instruction, and were sequenced on an Illumina HiSeq 2000 at the Mayo Clinic Center for Individualized Medicine Medical Genomics Facility. For qRT-PCR, transcription into cDNA was performed using random hexamer and SuperScript III reverse transcriptase (Invitrogen) according to the manufacturer's description. All PCR reactions was analyzed on a Bio-Rad real-time PCR machine with iQ^{TM} SYBRgreen PCR mastermix (Bio-Rad) to a final volume of 12 µl. Primer sequences used for qRT-PCR in this study are provided in Table S3.

Senescence assays

OIS IMR90s and oxidative-stressed MEFs were collected at different days/passages of induction, and cellular senescence was analyzed by measuring SA-β-gal activities, EdU incorporation, and formation of senescence-induced heterochromatin foci. Detection of SA-β-gal activity was performed using a Senescence β-Galactosidase Staining Kit (Cell Signaling Technology, # 9860) following the manufacturer's protocol. Images were captured by a fluorescence microscope Leica DM 4000 equipped with HC plan APO

20x/0.7 objective, DFC 450C color camera and LAS V4.4 software (Leica, IL, USA). For cell cycle arrest analyses, cells were labeled with EdU (5-ethyl-2'-deoxyuridine) using the Click-it EdU Alexa Fluor 555 imaging kit (Invitrogen). Briefly, 13 hrs after changing the medium, EdU was added at a final concentration of 10 μM, and 3 hrs later the cells were fixed for fluorescence staining of EdU, followed by DAPI for nuclear staining. Deoxyuridine incorporation was revealed with click-it chemistry according to the manufacturer's instructions. DAPI (1:2000, Sigma-Aldrich) was used to visualize SAHF. Each experiment was repeated three times, and about 200 cells were counted for each replicate.

H3.3-SNAP staining

Detection of new H3.3 deposition using the SNAP staining was performed as described previously (7-10). Briefly, 10 μM SNAP block reagent (New England Biolabs) was added to culture medium at 37°C for 30 min to quench old H3.3-SNAP in IMR90 cells. Cells were then washed with fresh medium three times and incubated in fresh medium for another 30 min. After chasing for 8 h, 2 μM SNAP-TMR-Star (New England Biolabs), a red fluorescent substrate, was added to the medium for 20 min at 37°C. Cells were then pre-extracted with 0.5% Triton-X100 (Sigma) and fixed in 3% paraformaldehyde. A fluorescence microscope (40 x) was used to record fluorescent images of SNAP staining and ImageJ software was used to quantify the SNAP fluorescence intensity. For each experiment, over 200 cells were counted.

Chromatin immunoprecipitation PCR (ChIP-PCR)

IMR90$^{ER:H\text{-}RasV12}$ cells were fixed with 1% formaldehyde for 10 min, followed by quenching with 125mM glycine and washed with cold TBS twice. Cells were resuspended in cell lysis buffer (10 mM Tris-HCl, pH7.5, 10mM NaCl, 0.5% NP-40) and then incubated on ice for 10 mins. Lysates were washed and resuspended in 500 µl Mnase digestion buffer (20 mM Tris-HCl, pH 7.5, 15 mM NaCl, 60 mM KCl, 1 mM CaCl2) with MNase (NEB, M0247S, 0.5U/1000 cells). After 20 minutes of incubation at 37°C with continuous mixing, digestion was stopped with 500 µl of sonication buffer (100 mM Tris-HCl, pH8.1, 20 mM EDTA, 200 mM NaCl, 2% Triton X-100, 0.2% sodium deoxycholate). Samples were sonicated for 7 cycles (30 secs on/30 secs off, Diagenode Bioruptor). Chromatin content was estimated by Qubit assay. 10µg chromatin were incubated with 0.3µg of H3.3 antibody (Diagenode, cat No. C15210011) for overnight at 4 °C. Antibody-bound complexes were then captured by incubation with 30µl of protein G-magnetic beads for 3 hr at 4 °C. The beads were washed extensively with ChIP buffer (50 mM Tris-HCl, pH8.1, 10 mM EDTA, 100 mM NaCl, 1% Triton X-100, 0.1% sodium deoxycholate), high salt buffer (50 mM Tris-HCl, pH8.1, 10 mM EDTA, 500 mM NaCl, 1% Triton X-100, 0.1% sodium deoxycholate), LiCl2 buffer (10 mM Tris-HCl, pH8.0, 0.25 M LiCl2, 0.5% NP-40, 0.5% sodium deoxycholate, 1 mM EDTA), and TE buffer. Bound DNA was eluted and reverse-crosslinked at 65°C overnight. After the treatment with RNase A and proteinase K, DNA was purified using a MiniElute PCR purification kit (Qiagen) and enrichment analyzed by q-PCR. Primer sequences used for ChIP-PCR in this study are provided in Table S3.

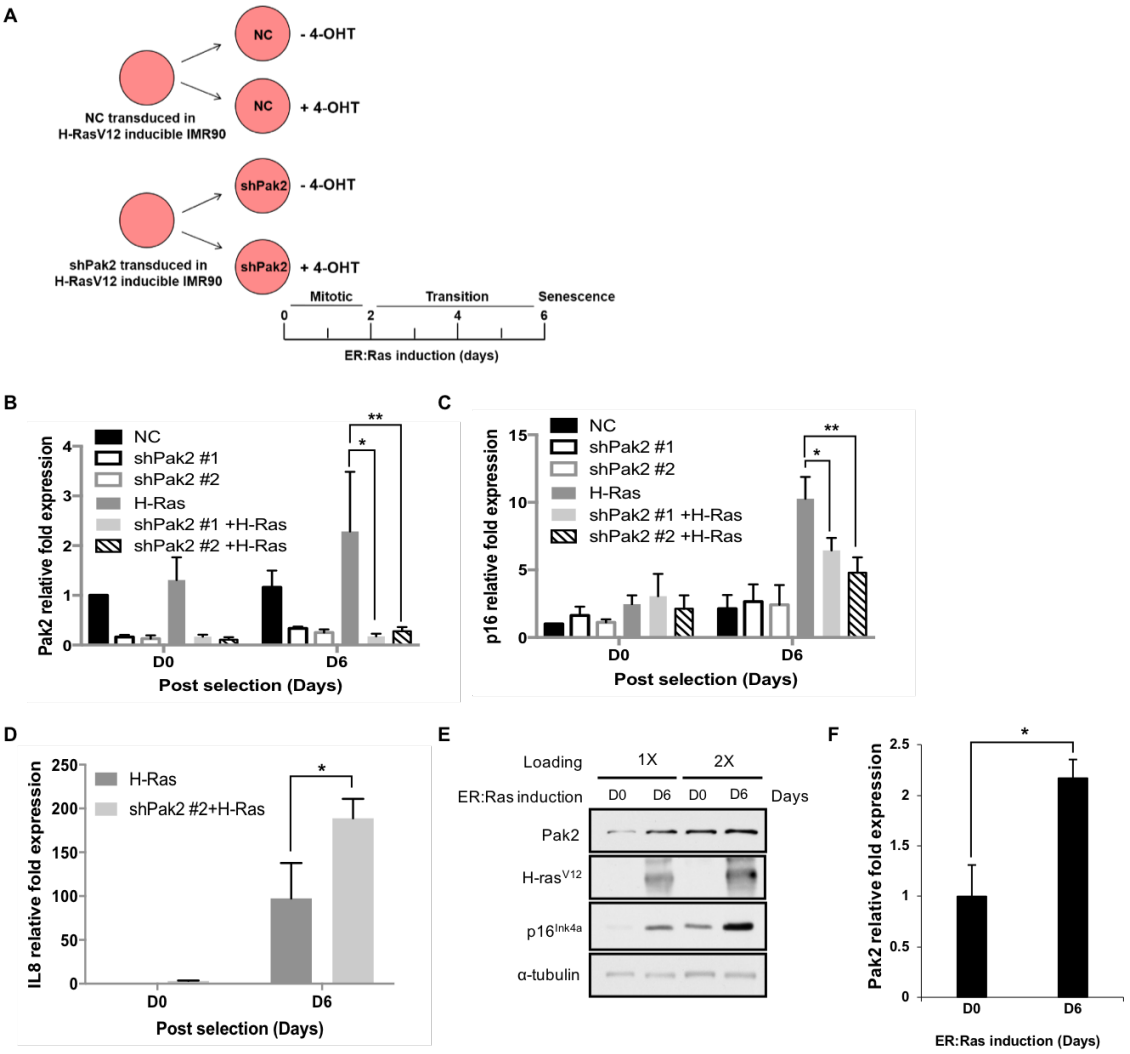

Fig. S1. Pak2 expression level increases in IMR90 cells during oncogene-induced senescence (OIS), and Pak2 depletion attenuates OIS. (A) Experimental design and time frame. After infection with virus against a non-targeting control (NC) or Pak2 (shPak2) and drug selection, IMR90 cells were treated with 4-hydroxytamoxifen (4OHT) to induce expression of H-RasV^{12}. Cellular senescence was monitored over six days. (B) Pak2 mRNA and (C) p16^{INK4a} mRNA level was determined by qRT-PCR (n=3, mean ± SEM, * $p<0.05$, ** $p<0.01$) using two independent shRNAs targeting Pak2 (indicated as #1 and #2). Relative fold expression was calculated by normalizing to day 0 (D0) non-target control values. (D) IL-8 mRNA level was determined by qRT-PCR (n=3, mean ± SEM, *

$p<0.05$) (E-F) Analysis of Pak2 expression level in IMR90 cells undergoing senescence. (E) Pak2 protein expression level was tested by Western blotting using lysates from IMR90 cells induced with H-RasV^{12} at D0 and D6. α-tubulin was used as a loading control. (F) Pak2 mRNA level was determined by qRT-PCR (n=3, mean ± SEM, * $p<0.05$). Value were normalized to GAPDH.

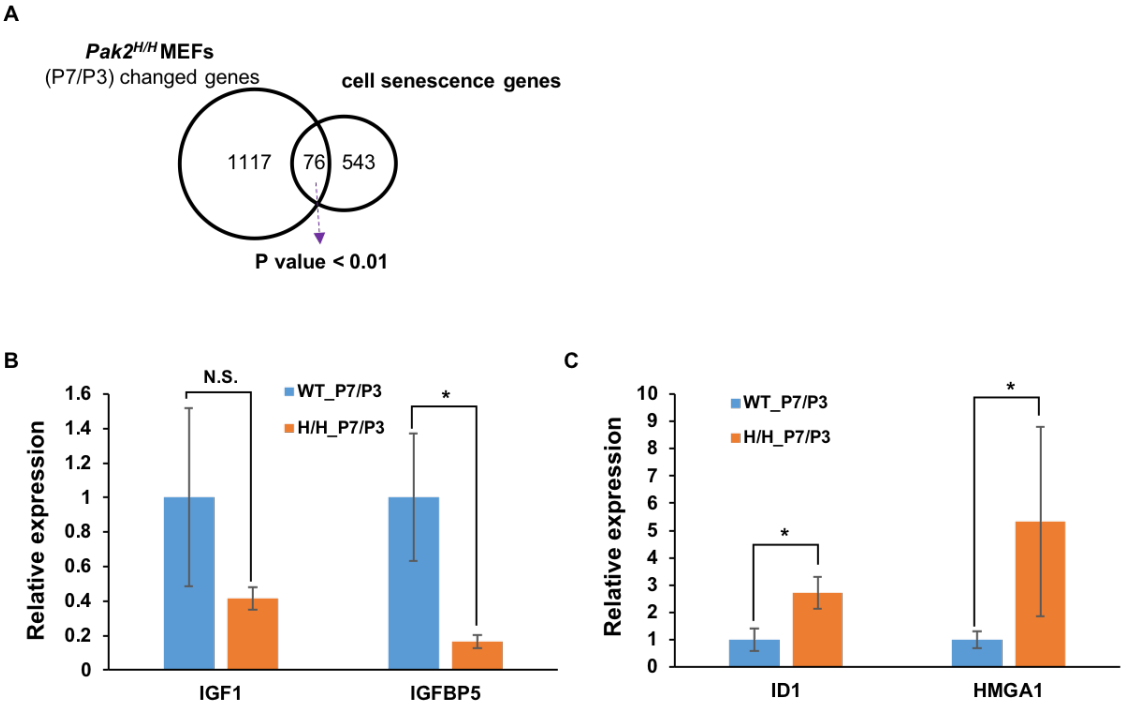

Fig. S2. Pak2 is required for the expression of cellular senescence genes. (A) Venn diagram showing the overlap between genes that are altered during senescence of Pak2$^{H/H}$ MEFs and those associated with cell senescence (gene set from CSGene and Ingenuity Pathway Analysis). (B-C) qRT-PCR analysis for relative expression of IGF1, IGFBP5, ID1, and HMGA1 during the passage of Pak2 WT and Pak2$^{H/H}$ MEF cells. Values were normalized to GAPDH and then normalized to WT MEFs to obtain relative expression (n=3 for each genotype, mean ± SEM, * $p<0.05$, N.S., not significant)

A

Genotype (n)	Age (weeks)	Fat%
WT (8)	16	14.92
$Pak2^{WT}$;$BubR1^{HH}$ (12)	16	11.32
$Pak2^{HH}$;$BubR1^{HH}$ (12)	16	14.03

*

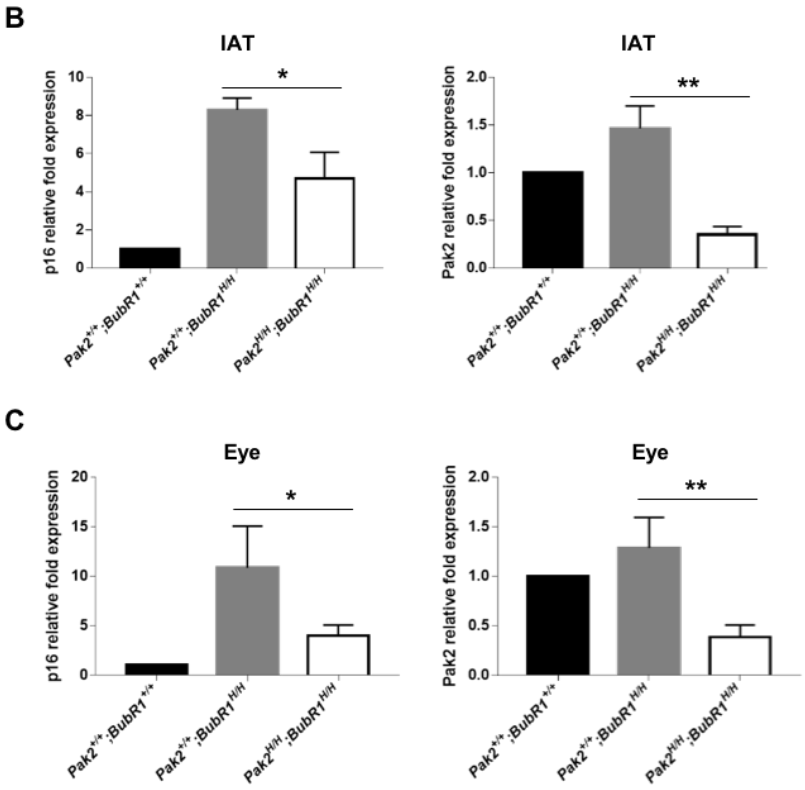

Fig. S3. Pak2 depletion delays the onset of aging phenotypes and increases lifespan in a mouse model of accelerated aging. (A) Analysis of body fat mass in *Pak2*$^{+/+}$;*BubR1*$^{H/H}$, *Pak2*$^{-/-}$;*BubR1*$^{H/H}$, and wildtype mice. The overall amount of fat was measured using quantitative nuclear magnetic resonance on live 16 week-old *Pak2*$^{+/+}$;*BubR1*$^{H/H}$, *Pak2*$^{-/-}$;*BubR1*$^{H/H}$ and wildtype mice. An unpaired t-test was applied for statistical analysis. * $p<0.05$. (B-C) qRT-PCR analysis for relative expression of $p16^{INK4a}$ and Pak2 in fat (B) and eye (C) from 4 months old *Pak2*$^{+/+}$;*BubR1*$^{H/H}$, *Pak2*$^{-/-}$;*BubR1*$^{H/H}$, and wildtype mice.

Values were normalized to GAPDH, and the relative fold expression to wildtype was reported (n=4 for each tissue, mean ± SEM, * $p<0.05$, ** $p<0.01$)

Additional data table S1 (separate file)

Table S1. Senescence associated genes list in Pak2 WT and Pak2$^{H/H}$ MEFs

Table S2. E2F target genes list from Pak2 WT and Pak2$^{H/H}$ MEFs RNA-seq data

E2F target Genes	p3_wt_FPKM	p3_homo_FPKM	p7_wt_FPKM	p7_homo_FPKM	Cell Function
Ccnd3	36.6591	30.124	13.7089	18.7649	G1
E2f1	14.0014	7.94058	11.1778	17.3958	G1/S Cell cycle
Ccne2	2.05923	3.23087	0.463895	0.848142	G1/S Cell cycle
Cdk2	6.10392	5.18953	2.24822	3.05057	G1/S Cell cycle
Mybl2	4.73603	5.77928	0.96685	2.84247	G1/S Cell cycle
Tfdp1	61.4372	48.9762	29.9686	37.2283	G1/S Cell cycle
Aurkb	14.2607	18.7536	4.06171	5.13631	S/G2 Cell cycle
Ccna2	36.3415	47.5373	8.27398	12.5516	S/G2 Cell cycle
Cks2	31.512	28.7989	4.88446	9.01818	S/G2 Cell cycle
Cdc20	23.453	17.4597	3.07083	6.05341	S/G2 Cell cycle
Prc1	29.1185	26.9194	5.92158	9.83223	S/G2 Cell cycle
Cdt1	5.2884	4.92426	1.62369	2.62994	DNA synthesis and replication
Dck	9.68541	8.29836	4.89277	6.95748	DNA synthesis and replication
Dut	13.443	11.6434	3.76462	6.01007	DNA synthesis and replication
Mcm3	19.7942	18.0523	6.32945	7.5222	DNA synthesis and replication
Mcm4	23.7228	23.6272	6.5063	8.91173	DNA synthesis and replication
Mcm5	7.90058	8.14586	2.10272	2.53046	DNA synthesis and replication
Mcm6	60.387	54.3396	21.2778	25.024	DNA synthesis and replication
Mcm7	19.0864	18.6825	6.31975	9.81904	DNA synthesis and replication
Pola2	9.10251	7.9903	3.09099	5.98841	DNA synthesis and replication
Rpa1	26.0621	17.014	8.42023	10.3949	DNA synthesis and replication
Rpa2	8.74809	6.58215	3.00699	6.47112	DNA synthesis and replication
Rpa3	12.1366	12.0736	4.21063	7.12873	DNA synthesis and replication
Rrm1	52.1813	44.7999	16.7547	21.5524	DNA synthesis and replication
Rrm2	77.5858	49.4593	16.1882	22.6781	DNA synthesis and replication
Bub1	9.78716	13.5933	2.01308	2.34037	Checkpoints
Bub1b	12.2641	14.9249	3.36836	5.13479	Checkpoints
Bub3	38.1903	23.875	16.0648	19.1447	Checkpoints
Bard1	2.54369	2.5788	0.835809	2.1909	DNA damage repair
Cstf1	9.6498	8.15807	2.84756	5.00726	DNA damage repair
Pms2	4.92212	4.69291	2.1452	3.47384	DNA damage repair
Rad51	9.80478	9.3306	3.36113	4.85394	DNA damage repair

Table S3. The sequences of primer pairs used for qRT-PCR and ChIP-PCR

Primers used for qRT-PCR	Sequences (5'-3')	Organism
GAPDH-Forward	GGACCTGAC CTGCCGTCTAGAA	Human
GAPDH-Reverse	GGTGTCGCTGTTGAAGTCAGAG	Human
β-actin-Forward	AGAGCTACGAGCTGCCTGAC	Hunam
β-actin-Reverse	AGCACTGTGTTGGCGTACAG	Hunam
Pak2-Forward	ACCCTGTTCCTGCACCAGTTGG	Hunam
Pak2-Reverse	ACTGTACCAGAAGCCCCTTG	Hunam
p16-Forward	TGCCCAACGCACCGAATAGT	Hunam
p16-Reverse	CAGCAGCTCCGCCACTCG	Hunam
IL6-Forward	TTCGGTCCAGTTGCCTCTC	Hunam
IL6-Reverse	TGGCATTTGTGGTTGGGTCA	Hunam
IL8-Forward	AAGAGAGCTCTGTCTGGACC	Hunam
IL8-Reverse	GATATTCTCTTGGCCCTTGG	Hunam
mGAPDH-Forward	TGGCAAAGTGGAGATTGTTGCC	Mouse
mGAPDH-Reverse	AAGATGGTGATGGGCTTCCCG	Mouse
mIgf1-Forward	AGACAGGCATTGTGGATGAG	Mouse
mIgf1-Reverse	TGAGTCTTGGGCATGTCAGT	Mouse
mIgfbp5-Forward	CGTGCTGTGTACCTGCCCAA	Mouse
mIgfbp5-Reverse	ACACCAGCAGATGCCACGTT	Mouse
mId1-Forward	CCCACTGGACCGATCCGCCA	Mouse
mId1-Reverse	TGCTCTCGGTTCCCCAGGGG	Mouse
mHmga1-Forward	CAAGCAGCCTCCGGTGAGTC	Mouse
mHmga1-Reverse	TTGGCGGCGCCCTTATTCTT	Mouse

Primers used for ChIP-PCR	Sequences (5'-3')	Organism
p16-TSS-Forward	ACCCCGATTCAATTTGGCAG	Hunam
p16-TSS-Reverse	AAAAAGAAATCCGCCCCCG	Hunam
IL6-enhancer-Forward	GTCTCTAGCAGAGAGGAAGGAGA	Hunam
IL6-enhancer-Reverse	TGACTTGGGAGGCAGGATTTC	Hunam

TSS indicates the transcription start site.

References

1. Kuilman T*, et al.* (2008) Oncogene-induced senescence relayed by an interleukin-dependent inflammatory network. *Cell* 133(6):1019-1031.
2. Duarte LF*, et al.* (2014) Histone H3.3 and its proteolytically processed form drive a cellular senescence programme. *Nature communications* 5:5210.
3. Corpet A, Olbrich T, Gwerder M, Fink D, & Stucki M (2014) Dynamics of histone H3.3 deposition in proliferating and senescent cells reveals a DAXX-dependent targeting to PML-NBs important for pericentromeric heterochromatin organization. *Cell cycle* 13(2):249-267.
4. McCurrach ME & Lowe SW (2001) Methods for studying pro- and antiapoptotic genes in nonimmortal cells. *Methods Cell Biol* 66:197-227.
5. Baker DJ*, et al.* (2004) BubR1 insufficiency causes early onset of aging-associated phenotypes and infertility in mice. *Nature genetics* 36(7):744-749.
6. Babu JR*, et al.* (2003) Rae1 is an essential mitotic checkpoint regulator that cooperates with Bub3 to prevent chromosome missegregation. *J Cell Biol* 160(3):341-353.
7. Ray-Gallet D*, et al.* (2011) Dynamics of histone H3 deposition in vivo reveal a nucleosome gap-filling mechanism for H3.3 to maintain chromatin integrity. *Molecular cell* 44(6):928-941.
8. Han J*, et al.* (2013) A Cul4 E3 ubiquitin ligase regulates histone hand-off during nucleosome assembly. *Cell* 155(4):817-829.
9. Zhang H, Wang Z, & Zhang Z (2013) PP1alpha, PP1beta and Wip-1 regulate H4S47 phosphorylation and deposition of histone H3 variant H3.3. *Nucleic Acids Res* 41(17):8085-8093.
10. Lee JS & Zhang Z (2016) O-linked N-acetylglucosamine transferase (OGT) interacts with the histone chaperone HIRA complex and regulates nucleosome assembly and cellular senescence. *Proceedings of the National Academy of Sciences of the United States of America* 113(23):E3213-3220.